

BER Analysis of Dual-Hop Relaying with Energy Harvesting in Nakagami- m Fading Channel

Mohammadreza Babaei, *Student Member, IEEE*, Ümit Aygözü, *Member, IEEE*,
and Ertugrul Basar, *Senior Member, IEEE*

Abstract—In this paper, the end-to-end bit error performance of a dual-hop (DH) energy harvesting (EH) amplify-and-forward/decode-and-forward (AF/DF) system is investigated. In this system, the source communicates with the destination over an intermediate relay when the direct link between the source and the destination is in deep fade. The channels are assumed to be exposed to Nakagami- m fading and all nodes are equipped with one antenna. The relay uses power splitting (PS) and time switching (TS) relaying protocols to harvest energy and uses it to forward the decoded signal or to transmit the amplified version of the received signal to the destination. The bit error probabilities (BEP) of the considered DH-AF and DH-DF systems are analytically derived for both EH protocols and their performances are comparatively evaluated. Moreover, a system optimization is performed to maximize the BER performance. For the TS mode, a list of mixture of modulations is provided for different spectral efficiency values and different time allocation parameters. Our comprehensive results on the BER performance of AF- and DF-aided DH networks with EH in the relay, provide basic guidelines for the design of future DH-EH systems.

Index Terms—Energy harvesting, dual-hop network, DF/AF relaying, performance analysis.

I. INTRODUCTION

ENERGY harvesting (EH) from radio frequency (RF) signals is a promising approach that has been regarded as an alternative solution to the power efficiency issue [1], [2]. In EH, nodes can both harvest energy and process the information concurrently. As a result, the EH node does not need to have an external source of energy since it uses the harvested energy to forward the received signal to a destination. In the literature, practical EH techniques are classified as power splitting (PS) and time switching (TS) relaying. In PS, the EH node divides the incoming signal power in two parts for EH and information processing (IP) during the whole transmission interval. In TS, a certain fraction of the transmission interval is reserved to EH while the remainder fraction to IP. For both protocols, EH

node uses the harvested energy to transmit the received signal to its destination. On the other hand, an ideal (unrealistic) EH node, which is commonly considered in the literature [2]–[4], simultaneously harvests energy and processes information with the total received power.

A dual-hop decode-and-forward (DH-DF) relaying network, where the relay applies PS and TS protocols, is considered in [5] and the achievable throughput at the destination is derived from ergodic capacity. In [6], the outage performance of an amplify-and-forward (AF) cooperative EH system is derived when the source has the knowledge of channel statistics. Given a total power constraint for the whole system, the TS parameter is optimized to improve TS performance compared to PS. In [3], the outage probability and ergodic capacity of delay-limited and delay-tolerant transmission schemes are derived for the DH-AF relaying strategy by considering PS, TS and ideal EH protocols. Overall sum bit error rate (BER) in a two-way physical layer network coding AF relaying system is derived for two and three transmission intervals in [7] where the relay harvests energy applying TS. Moreover, the mixture of modulations approach is proposed in [7] to maintain the spectral efficiency at a fixed value when the TS parameter α varies and the BER performance is analytically evaluated for fixed spectral efficiency values. An adaptive EH protocol in a half duplex AF transmission system applying TS and PS protocols together is considered in [8], where the system throughput is obtained by deriving expressions for the outage probability and ergodic capacity. The results are compared with the conventional PS and TS protocols and it is concluded that the adaptive EH protocol provides better performance in moderate transmission rates where the throughput curves of PS and TS cross over each other. In [9], a source communicates with a destination via an EH relay in which the channels are exposed to Nakagami- m fading and all nodes are equipped with multiple antennas. The system throughput is derived for both PS and TS where transmit/receive antenna selection and maximum ratio transmitter/maximum ratio combiner (MRT/MRC) are employed for each hop. Achievable rate for the DH-AF relaying system, in which the relay is equipped with multiple antennas, is studied in [10]. The relay uses antenna selection (AS) and PS to decode the information and harvests energy. Moreover, an optimization is jointly effectuated for AS and PS to improve the system performance. PS and TS protocols are considered in [11] to analyze the performance of a DH system with DF relaying. In [11], the relay harvests energy from both the received signal and the interference signals at the same frequency, which in fact

Manuscript received November 8, 2017; revised February 12, 2018; accepted April 1, 2018. Date of publication XXXXX X, 2018; date of current version XXXXX X, 2018. This paper was partly presented at the 2017 Advances in Wireless and Optical Communications, Riga, Latvia, November 2017. This work was supported by the Scientific and Technological Research Council of Turkey (TUBITAK) under Grant 114E607. The work of E. Basar was also supported by Turkish Academy of Sciences (TUBA) Outstanding Young Scientist Award Programme (GEBIP). The associate editor coordinating the review of this paper and approving it for publication was Rui Dinis.

The authors are with the Department of Electronics and Communication Engineering, Istanbul Technical University, Maslak, 34469, Istanbul, Turkey, E-mails: (babaei, aygolu, basarer)@itu.edu.tr.

Color versions of one or more of the figures in this paper are available online at <http://ieeexplore.ieee.org>.

Digital Object Identifier 10.1109/TWC.2018.XXXXXXX

increases the relay transmission power. However, this causes a decrease in the relay's received signal-to-noise ratio (SNR). A dynamic power splitting (DPS) receiver operation, which splits the signal power for IP and EH, is proposed in [4]. TS, static PS and on-off PS are studied as the special cases of DPS. Moreover, integrated and separated practical information and EH receivers are presented in [4].

In [12], a wireless powered communication network is proposed for which the source itself is a power-constraint node and harvests energy from the energy transmitters. The relays or destination have constant powers and the source transmits data to the destination with the harvested energy. In [12], two different protocols are proposed and jointly optimized to maximize the throughput for EH. In the first protocol, the relay cooperates only to transfer energy to the source. However, in the second protocol, the relay not only transmits energy to the power-constraint source but also it forwards the received signal from the source to the destination in order to improve the system performance.

An energy harvesting system with spatial modulation is considered in [13] where a PS receiver architecture is assumed at the receiver. Computational complexity of this system has been analyzed and the optimal PS factor is determined to maximize the system throughput. Another EH system with SM, in which the source harvests RF energy from an energy transmitter, has been analyzed in [14]. The source is equipped with multiple antennas in which some of them are active during the information transmission, and this enables self-energy recycling at the antennas, which provides more harvested energy at the source node.

Two-way relaying (TWR) EH systems are studied in [15]–[19]. In [15] and [16], TS and AF are considered. Throughput from the outage probability and ergodic capacity are derived in the Nakagami- m fading channel in [15]. Moreover, the MRT/MRC technique is applied at the source and destination. In [16], bidirectional multiple access broadcast and time division broadcast techniques are proposed. Furthermore, three power transfer policies are investigated at the sources. In [17] and [18], a TW system with PS architecture is considered. In [17], the energy efficiency optimization problem under the rate and total power constraints is studied. In [18], a PS energy accumulation scheme in a TWR system is considered, in which the relay is assumed to be a power-constraint unit and equipped with a rechargeable battery. If the amount of energy at the relay battery reaches a predefined threshold, the relay applies PS and forwards the signal to the destination. However, if the energy is below the threshold level, the relay harvests all of the received signal energy in its battery. In [19], the performance of a three-step DF system, in which PS is used at the relay, is analyzed where bidirectional communication of two sources is allowed.

EH systems are mostly studied in the literature from the outage performance perspective. To the best of our knowledge, the bit error performance of DH-(AF/DF) relaying systems with an EH relay in Nakagami- m fading channels as well as comparisons between various EH protocols have not been studied in the literature yet.

In this paper, bit error performance of the DH system with

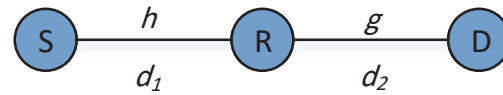


Fig. 1. Considered dual-hop system.

an EH relay is investigated. For the AF relaying system, the relay harvests energy from the received RF source signal and then using the harvested energy, it forwards the noisy version of the received signal to the destination. For the DF relaying system, the relay decodes and harvests the source signal and then using the harvested energy, transmits the decoded source signal to the destination. For AF/DF relaying strategies, PS, TS and ideal EH protocols are considered. Bit error probability (BEP) of the system is analytically derived for the aforementioned EH protocols under AF/DF strategies. Computer simulations are performed for different system parameters and the results are found in perfect match with those analytically obtained.

The main contributions of this paper are summarized as follows:

- BER analysis of PS, TS and ideal operational EH protocols in a DH network with a power constraint relay, which enables wireless energy harvesting and information processing simultaneously, is derived.
- A unified BEP analysis is presented for the PS, TS and ideal protocols.
 - An upper bound on the end-to-end BEP is evaluated for the DH-DF system.
 - End-to-end BEP for the DH-AF system is derived using CDF of the received SNR.
- Results are given for different system parameters. Moreover, the optimum system parameters minimizing the BEP are determined.
- BER performance comparisons between AF and DF relaying EH systems are provided.
- To make a fair comparison between TS and the other protocols, on an equal spectral efficiency basis, the idea of mixture of modulations given previously in [7] is generalized for different spectral efficiency values.

The rest of the paper is organized as follows. In Section II, the considered system model is presented. Section III is destined to the BEP analysis and in Section IV, theoretical and computer simulation results are presented. Finally, Section V concludes the paper.

II. SYSTEM MODEL

The considered dual-hop system model is given in Fig. 1 where all nodes are equipped with one antenna. h and g represent the channel fading coefficients between links S→R and R→D, respectively. d_1 and d_2 denote the link distances. Both channels are assumed to be exposed to Nakagami- m fading. In the sequel, s and \bar{s} stand for the transmitted signal from the source and the decoded signal at the relay, respectively. Moreover, it is assumed that $E\{|s|^2\} = E\{|\bar{s}|^2\} = 1$. n_r and n_d denote additive white Gaussian noise (AWGN) samples at the relay and the destination with distributions

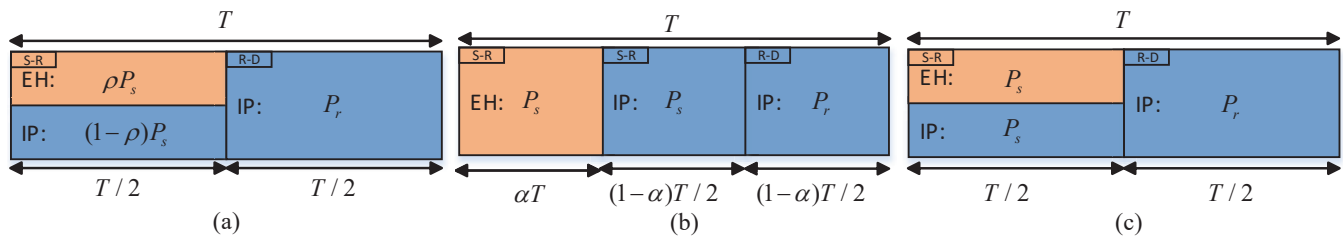


Fig. 2. Time schedule for (a) PS protocol, (b) TS protocol and (c) ideal protocol.

$n_r \sim \mathcal{CN}(0, \sigma_r^2)$ and $n_d \sim \mathcal{CN}(0, \sigma_d^2)$, respectively. Note that since the system performance is analyzed for distances d_1 and d_2 , which are smaller than unity, the path-loss for both links S \rightarrow R and R \rightarrow D are assumed to be equal to $L_{SR} = 1/(1 + d_1^\xi)$ and $L_{RD} = 1/(1 + d_2^\xi)$, respectively, to ensure that the path loss is always smaller than unity for any distance, where ξ is the path-loss coefficient [20]. P_s is the source transmit power, P_r is the relay transmit power and P_t is the average power consumed by the system during T seconds. Moreover, Gray mapping is applied for all modulation schemes performed at the source and relay transmitters¹.

A. DF Relaying

1) *DF-PS EH Protocol*: Transmission time schedule for the PS protocol is given in Fig. 2(a). As shown in Fig. 2(a), in PS protocol, the power of received signal at the relay is divided into EH and IP operations with the energy proportion of $\rho/(1-\rho)$, where ρ is the power harvesting factor. In the first time interval of $T/2$ seconds, the received signal for IP and the harvested energy at the relay are given as

$$y_r = \sqrt{(1-\rho)P_s L_{SR}} h s + n_r \quad (1)$$

and

$$E_H = \eta \rho P_s L_{SR} |h|^2 (T/2) \quad (2)$$

respectively, where $0 < \eta \leq 1$ is the energy conversion coefficient [4]. Considering the total power-constraint P_t for the system and the energy constraint $P_t T = P_s T/2$, we have $P_s = 2P_t$.

In the second time interval, the relay forwards the decoded signal \bar{s} to the destination using the harvested energy E_H . The received signal at the destination can be expressed as

$$y_d = \sqrt{P_r L_{RD}} g \bar{s} + n_d \quad (3)$$

where $P_r = E_H/(T/2) = \eta \rho P_s L_{SR} |h|^2$.

2) *DF-TS EH Protocol*: From the transmission time schedule given in Fig. 2(b) for TS protocol, in the first and second time intervals of duration αT and $(1-\alpha)T/2$ seconds, respectively, the received signal at the relay is given by

$$y_r = \sqrt{P_s L_{SR}} h s + n_r \quad (4)$$

¹Notation: $\text{erfc}(z) = (2/\sqrt{\pi}) \int_z^\infty e^{-t^2} dt$ is the complementary error function [21, (8.250-4)], $W_{p,q}(\cdot)$ is the Whittaker function [21, (9.220-4)], $\Gamma(\cdot)$ is the Gamma function [21, (8.310-1)], $G_{p,q}^{m,n} \left(\begin{matrix} a_p \\ b_q \end{matrix} \right)$ represents Meijer's G-Function [21, (9.301)] and $K_\nu(\cdot)$ represents the ν^{th} -order modified Bessel function of the second kind [21, (8.432)].

where for αT seconds, the harvested amount of energy at the relay is $E_H = \eta P_s L_{SR} |h|^2 \alpha T$. Assuming that a total power of P_t is consumed in T seconds, the energy constraint for TS is given as

$$P_t T = P_s \alpha T + P_s (1-\alpha) T/2. \quad (5)$$

After simplifying, we have $P_s = 2P_t/(1+\alpha)$.

In the third time interval of $(1-\alpha)T/2$ seconds, the relay forwards the decoded signal to the destination for which the received signal is as given in (3), where

$$P_r = 2E_H/(1-\alpha)T = \eta(2\alpha/(1-\alpha))P_s L_{SR} |h|^2.$$

3) *DF-Ideal EH Protocol*: The time schedule for the ideal EH protocol is given in Fig. 2(c), where during the first time interval of $T/2$ seconds, the relay harvests energy and processes the information from the received source signal with the same total received energy. In the next time interval of $T/2$ seconds, the decoded signal is transmitted from the relay antenna to the destination node using the harvested energy. The received signal at the relay and the destination are given as in (4) and (3), respectively. For this protocol, $E_H = \eta P_s L_{SR} |h|^2 (T/2)$, the relay power is given as $P_r = 2E_H/T = \eta P_s L_{SR} |h|^2$ and like PS, $P_s = 2P_t$.

B. AF Relaying

In AF relaying strategy, the received signal at the relay is normalized, amplified and then retransmitted from the relay to the destination. Similar to DF relaying, three different EH protocols are analyzed in the following.

1) *AF-PS EH Protocol*: Using the received signal y_r at the relay given by (1), the received signal at the destination is expressed as

$$y_d = \sqrt{(P_r L_{RD}/N)} g y_r + n_d \quad (6)$$

where $N = P_s |h|^2 (1-\rho) L_{SR} + \sigma_r^2$ is a power constraint factor applied at the relay. Substituting (1) in (6) and after some simplification, we have

$$y_d = \frac{\sqrt{\eta |h|^2 \rho (1-\rho)} P_s h g s}{\sqrt{(1+d_1^\xi)(1+d_2^\xi)} \sqrt{P_s |h|^2 (1-\rho) + (1+d_1^\xi) \sigma_r^2}} + \frac{\sqrt{\eta P_s |h|^2 \rho g n_r}}{\sqrt{1+d_2^\xi} \sqrt{P_s |h|^2 (1-\rho) + (1+d_1^\xi) \sigma_r^2}} + n_d. \quad (7)$$

2) *AF-TS EH Protocol*: The received signal at the destination is given as

$$y_d = \sqrt{(P_r L_{RD}/J)} g y_r + n_d \quad (8)$$

where $J = P_s |h|^2 L_{SR} + \sigma_r^2$. Substituting (4) in (8) and after some simplification, we obtain

$$y_d = \frac{\sqrt{2\eta|h|^2 \alpha} P_s h g_s}{\sqrt{(1-\alpha)(1+d_1^\xi)(1+d_2^\xi)} \sqrt{P_s |h|^2 + (1+d_1^\xi) \sigma_r^2}} + \frac{\sqrt{2\eta P_s |h|^2 \alpha} g_n r}{\sqrt{(1-\alpha)(1+d_2^\xi)} \sqrt{P_s |h|^2 + (1+d_1^\xi) \sigma_r^2}} + n_d. \quad (9)$$

3) *AF-Ideal EH Protocol*: The received signal at the relay and destination are as given in (4) and (8), respectively. Substituting (4) in (8), considering $P_r = 2E_H/T = \eta P_s L_{SR} |h|^2$ and after some simplification, we have

$$y_d = \frac{\sqrt{\eta|h|^2} P_s h g_s}{\sqrt{(1+d_1^\xi)(1+d_2^\xi)} \sqrt{P_s |h|^2 + (1+d_1^\xi) \sigma_r^2}} + \frac{\sqrt{\eta P_s |h|^2} g_n r}{\sqrt{(1+d_2^\xi)} \sqrt{P_s |h|^2 + (1+d_1^\xi) \sigma_r^2}} + n_d. \quad (10)$$

III. BIT ERROR PROBABILITY ANALYSIS

A. BEP for DF Relaying

For the three-node DH relaying system given in Fig. 1, the relay decodes the received signal from the source and transmits the decoded symbol \bar{s} to the destination. The end-to-end BEP can be upper bounded as

$$P_b^{DF} \leq 1 - (1 - P_b^{S-R})(1 - P_b^{R-D}) \quad (11)$$

where P_b^{S-R} and P_b^{R-D} are BEPs of the links S→R and R→D, respectively, which are calculated for different EH protocols in the following.

From the received signals at the relay given in (1) for PS and in (4) for TS and ideal protocols, SNR of the link S→R can be written as

$$\gamma_{sr} \triangleq \begin{cases} (1-\rho)P_s L_{SR} |h|^2 / \sigma_r^2, & \text{PS} \\ P_s L_{SR} |h|^2 / \sigma_r^2, & \text{TS and ideal.} \end{cases} \quad (12)$$

Using (12) and the exact BEP of the link S→R given in [22, Chap. 8], P_b^{S-R} can be substituted in (11).

From the received signal at the destination given in (3), SNR of the link R→D for all EH protocols can be expressed as $\gamma_{rd} = \Upsilon Z$ where $Z = |h|^2 |g|^2$ and

$$\Upsilon \triangleq \begin{cases} \eta \rho P_s L_{SR} L_{RD} / \sigma_d^2, & \text{PS} \\ \eta 2\alpha P_s L_{SR} L_{RD} / ((1-\alpha)\sigma_d^2), & \text{TS} \\ \eta P_s L_{SR} L_{RD} / \sigma_d^2, & \text{ideal.} \end{cases} \quad (13)$$

From [23, (5-17)], PDF of γ_{rd} is given as

$$f_{\gamma_{rd}}(\gamma) = \frac{1}{\Upsilon} f_Z\left(\frac{\gamma}{\Upsilon}\right) = 2G\gamma^{\epsilon-1} K_\Omega \left(2\sqrt{\frac{m_h m_g}{\Omega_h \Omega_g \Upsilon}} \gamma\right) \quad (14)$$

where $G = F(m_g \Omega_h / \Omega_g m_h)^{\Omega/2} (1/\Upsilon)^\epsilon$. m_h , m_g , Ω_h , Ω_g , $\epsilon = 0.5(m_h + m_g)$, $\Omega = m_h - m_g$, F and $f_Z(z)$ are defined

in Appendix A. The symbol error probability (SEP) of the link R→D can be calculated as

$$P_s^{R-D} = \int_0^\infty P_s(e|\gamma_{rd}) f_{\gamma_{rd}}(\gamma) d\gamma \quad (15)$$

where $f_{\gamma_{rd}}(\gamma)$ is calculated in (14) and $P_s(e|\gamma_{rd}) \simeq a Q(\sqrt{2b\gamma_{rd}}) = (a/2) \operatorname{erfc}(\sqrt{b\gamma})$ is the conditional common approximate SEP for coherent modulation [22]. Here, a and b are modulation specific constants². Note that the given conditional SEP is a tight upper bound at high SNR. In order to solve the integral of (15), we express $\operatorname{erfc}(\cdot)$ and $K_\nu(\cdot)$ in terms of the Meijer's G-function using [25, (06.27.26.0006.01)] and [26, (14)]. Substituting in (15), the integral can be rewritten as follows

$$P_s^{R-D} = \frac{Ga}{2\sqrt{\pi}} \int_0^\infty \gamma^{\epsilon-1} G_{1,2}^{2,0} \left(b\gamma \left| \begin{matrix} 1 \\ 0, \frac{1}{2} \end{matrix} \right. \right) G_{0,2}^{2,0} \left(\frac{H^2}{4} \gamma \left| \begin{matrix} - \\ \Omega/2, -\Omega/2 \end{matrix} \right. \right) d\gamma \quad (16)$$

where $H = 2\sqrt{m_h m_g / \Omega_h \Omega_g \Upsilon}$. Using [21, (9.311)] and [26, (21)], the closed-form solution for the integral in (16) is obtained as

$$P_s^{R-D} = \frac{Ga}{2\sqrt{\pi}} b^{-\epsilon} G_{4,5}^{3,3} \left(\frac{H^2}{4b} \left| \begin{matrix} 0, 1-\epsilon, 0.5-\epsilon, 1-\epsilon \\ 0.5\Omega, -0.5\Omega, 1-\epsilon, -\epsilon, 0 \end{matrix} \right. \right). \quad (17)$$

BEP for the link R→D can be obtained using the common approximation [22] at high SNR as

$$P_b^{R-D} \simeq P_s^{R-D} / k \quad (18)$$

where $k = \log_2 M$ and M is the modulation level. The end-to-end BEP can be upper bounded by substituting P_b^{S-R} and P_b^{R-D} from [22, Chap. 8] and (18), in (11), respectively.

It is important to note from (17) that the end-to-end BEP of the DF relaying system is dependent on the selected EH protocol through G and H terms, while modulation specific parameters a and b also affect the performance.

B. BEP for AF Relaying

The end-to-end SNR of the received signals in (7), (9) and (10) is given as

$$\gamma = \frac{A|h|^4 |g|^2}{B|h|^2 |g|^2 + C|h|^2 + D} \quad (19)$$

where the constants A, B, C and D are listed in Table II for different EH protocols. The CDF of γ at high SNR, where $D = 0$, is calculated in Appendix B. BEP of the system can be obtained using the CDF of SNR given in (32) of Appendix B as [24]

$$P_b^{AF} \simeq \frac{a\sqrt{b}}{2k\sqrt{\pi}} \int_0^\infty \frac{e^{-b\gamma}}{\sqrt{\gamma}} F_\gamma(\gamma) d\gamma = \frac{a\sqrt{b}}{2k\sqrt{\pi}} (I_1 - I_2) \quad (20)$$

where the constants a and b are determined by the modulation order. In (20), using [21, (3.381)], I_1 is expressed as

$$I_1 = \int_0^\infty \frac{e^{-b\gamma}}{\sqrt{\gamma}} d\gamma = \frac{1}{\sqrt{b}} \Gamma\left(\frac{1}{2}\right) \quad (21)$$

²For rectangular M -QAM, $a = 4(1 - 1/\sqrt{M})$, $b = 3/2(M - 1)$, for non-rectangular M -QAM, $a = 4$, $b = 3/2(M - 1)$, for M -PSK, $a = 2$, $b = \sin^2(\pi/M)$ and for BPSK, $a = 1$, $b = 1$ [24].

TABLE I
MIXTURE OF MODULATIONS FOR TS PROTOCOL ($R = 0.5$ AND $R = 1$)

α	IP time/ T	$R = 0.5$	$R = 1$	α	IP time/ T	$R = 0.5$	$R = 1$
1/20	$\approx 1/2$	M_1	M_2	8/15	7/30	$(6/7)M_2, (1/7)M_3$	$(5/7)M_4, (2/7)M_5$
1/12	11/24	$(10/11)M_1, (1/11)M_2$	$(9/11)M_2, (2/11)M_3$	11/20	9/40	$(7/9)M_2, (2/9)M_3$	$(5/9)M_4, (4/9)M_5$
1/7	3/7	$(5/6)M_1, (1/6)M_2$	$(2/3)M_2, (1/3)M_3$	5/9	2/9	$(3/4)M_2, (1/4)M_3$	$(1/2)M_4, (1/2)M_5$
1/6	5/12	$(4/5)M_1, (1/5)M_2$	$(3/5)M_2, (2/5)M_3$	8/14	3/14	$(2/3)M_2, (1/3)M_3$	$(1/3)M_4, (2/3)M_5$
1/5	2/5	$(3/4)M_1, (1/4)M_2$	$(1/2)M_2, (1/2)M_3$	23/40	17/80	$(11/17)M_2, (6/17)M_3$	$(5/17)M_4, (12/17)M_5$
1/4	3/8	$(2/3)M_1, (1/3)M_2$	$(1/3)M_2, (2/3)M_3$	3/5	1/5	$(1/2)M_2, (1/2)M_3$	M_5
4/14	5/14	$(3/5)M_1, (2/5)M_2$	$(1/5)M_2, (4/5)M_3$	10/16	3/16	$(1/3)M_2, (2/3)M_3$	$(2/3)M_5, (1/3)M_6$
1/3	1/3	$(1/2)M_1, (1/2)M_2$	M_3	2/3	1/6	M_3	M_6
3/8	5/16	$(2/5)M_1, (3/5)M_2$	$(4/5)M_3, (1/5)M_4$	14/20	3/20	$(2/3)M_3, (1/3)M_4$	$(1/3)M_6, (2/3)M_7$
4/10	3/10	$(1/3)M_1, (2/3)M_2$	$(2/3)M_3, (1/3)M_4$	5/7	1/7	$(1/2)M_3, (1/2)M_4$	M_7
5/12	7/24	$(2/7)M_1, (5/7)M_2$	$(4/7)M_3, (3/7)M_4$	6/8	1/8	M_4	-
3/7	2/7	$(1/4)M_1, (3/4)M_2$	$(1/2)M_3, (1/2)M_4$	7/9	1/9	$(1/2)M_4, (1/2)M_5$	-
8/18	5/18	$(1/5)M_1, (4/5)M_2$	$(2/5)M_3, (3/5)M_4$	8/10	1/10	M_5	-
11/24	13/48	$(2/13)M_1, (11/13)M_2$	$(4/13)M_3, (9/13)M_4$	10/12	1/12	M_6	-
1/2	1/4	M_2	M_4	12/14	1/14	M_7	-

TABLE II
A, B, C AND D CONSTANTS

PS	A	$\eta \rho P_s^2 (1 - \rho)$
	B	$\eta \rho P_s (1 + d_1^\xi) \sigma_r^2$
	C	$(1 - \rho) P_s (1 + d_1^\xi) (1 + d_2^\xi) \sigma_d^2$
	D	$(1 + d_1^\xi)^2 (1 + d_2^\xi) \sigma_r^2 \sigma_d^2$
TS	A	$\eta \frac{2\alpha}{1 - \alpha} P_s^2$
	B	$\eta \frac{2\alpha}{1 - \alpha} P_s (1 + d_1^\xi) \sigma_r^2$
	C	$P_s (1 + d_1^\xi) (1 + d_2^\xi) \sigma_d^2$
	D	$(1 + d_1^\xi)^2 (1 + d_2^\xi) \sigma_r^2 \sigma_d^2$
ideal	A	ηP_s^2
	B	$\eta P_s (1 + d_1^\xi) \sigma_r^2$
	C	$P_s (1 + d_1^\xi) (1 + d_2^\xi) \sigma_d^2$
	D	$(1 + d_1^\xi)^2 (1 + d_2^\xi) \sigma_r^2 \sigma_d^2$

and

$$I_2 = \frac{2}{\Gamma(m_g)} \sum_{k=0}^{m_h-1} \sum_{i=0}^k T(k, i) I_3 \quad (22)$$

where

$$I_3 = \int_0^\infty \frac{e^{-b\gamma}}{\sqrt{\gamma}} \Lambda(k, i, \gamma) d\gamma. \quad (23)$$

Here, $T(k, i)$ and $\Lambda(k, i, \gamma)$ are defined in Appendix B. Considering the integral variable $\gamma = \delta^2$, $\Theta = \frac{m_h B}{\Omega_h A} + b$, $\varpi = \frac{m_g - i + 2k - 1}{2}$, $v = m_g - i$, $\beta = 2\sqrt{\frac{m_h m_g C}{\Omega_h \Omega_g A}}$ and using

[21, (6.631-3)] we have

$$I_3 = 2 \times 0.5 \Theta^{-0.5u} \beta^{-1} \Gamma\left(\frac{1+v+u}{2}\right) \Gamma\left(\frac{1-v+u}{2}\right) \times \exp\left(\frac{\beta^2}{8\Theta}\right) W_{-0.5u, 0.5v}\left(\frac{\beta^2}{4\Theta}\right) \quad (24)$$

where $u = 2\varpi + 1$ and the constants A, B, C and D are given in Table II. Substituting (24) in (22) and then I_1 and I_2 in (20), we finally obtain the BEP of the system.

As seen from (20), the BEP performance of AF relaying system is dependent on the considered EH protocol through only I_2 , which itself contains EH protocol dependent terms $T(k, i)$ and I_3 .

IV. PERFORMANCE EVALUATION

This section deals with theoretical and computer simulation-aided end-to-end BER results of the considered DH-(AF/DF) systems for different system parameters. Unless otherwise stated, we set the path loss exponent to $\xi = 2.7$, energy harvesting efficiency to $\eta = 1$ and $\Omega_h = \Omega_g = E[|h|^2] = E[|g|^2] = 1$. We consider $\sigma^2 = \sigma_r^2 = \sigma_d^2$. The source to destination distance is set to unity while the source to relay distance is assumed variant and the three nodes are co-linearly located. Moreover, in all figures, theoretical curves are denoted by straight lines and markers represent computer simulation results.

Unlike PS and ideal relaying for which the transmission time interval is fixed and equals to $T/2$, for the TS case, information processing time is variant and dependent on the parameter α , where αT and $(1 - \alpha)T$, respectively stand for EH and information processing time intervals in Fig. 2(b). As a result, BEP should be calculated only during the time interval of $(1 - \alpha)T$ in which the information processing time intervals for link $S \rightarrow R$ and $R \rightarrow D$ are equal to $(1 - \alpha)T/2$. On the other hand, for both PS and ideal EH relaying protocols, information processing time interval is equal to $T/2$ for each link (Figs. 2(a) and 2(c)). Consequently,

TABLE III
MIXTURE OF MODULATIONS FOR TS PROTOCOL ($R = 1.5$ AND $R = 2$)

α	IP time/ T	$R = 1.5$	$R = 2$
1/20	$\approx 1/2$	M_3	M_4
1/12	11/24	$(8/11)M_3, (3/11)M_4$	$(7/11)M_4, (4/11)M_5$
1/7	3/7	$(1/2)M_3, (1/2)M_4$	$(1/3)M_4, (2/3)M_5$
1/6	5/12	$(2/5)M_3, (3/5)M_4$	$(1/5)M_4, (4/5)M_5$
1/5	2/5	$(1/4)M_3, (3/4)M_4$	M_5
1/4	3/8	M_4	$(2/3)M_5, (1/3)M_6$
4/14	5/14	$(4/5)M_4, (1/5)M_5$	$(2/5)M_5, (3/5)M_6$
1/3	1/3	$(1/2)M_4, (1/2)M_5$	M_6
3/8	5/16	$(1/5)M_4, (4/5)M_5$	$(3/5)M_6, (2/5)M_7$
4/10	3/10	M_5	$(1/3)M_6, (2/3)M_7$
5/12	7/24	$(6/7)M_5, (1/7)M_6$	$(1/7)M_6, (6/7)M_7$
3/7	2/7	$(3/4)M_5, (1/4)M_6$	M_7
8/18	5/18	$(3/5)M_5, (2/5)M_6$	-
11/24	13/48	$(6/13)M_5, (7/13)M_6$	-
1/2	1/4	M_6	-
8/15	7/30	$(4/7)M_6, (3/7)M_7$	-
11/20	9/40	$(1/3)M_6, (2/3)M_7$	-
5/9	2/9	$(1/4)M_6, (3/4)M_7$	-
8/14	3/14	M_7	-

TABLE IV
MIXTURE OF MODULATIONS FOR TS PROTOCOL ($R = 2.5$ AND $R = 3$)

α	IP time/ T	$R = 2.5$	$R = 3$
1/20	$\approx 1/2$	M_5	M_6
1/12	11/24	$(6/11)M_5, (5/11)M_6$	$(5/11)M_6, (6/11)M_7$
1/7	3/7	$(1/6)M_5, (5/6)M_6$	M_7
1/6	5/12	M_6	-
1/5	2/5	$(3/4)M_6, (1/4)M_7$	-
1/4	3/8	$(1/3)M_6, (2/3)M_7$	-
4/14	5/14	M_7	-

to make a fair comparison between TS protocols and the other protocols such as ideal and PS, on an equal spectral efficiency basis, the idea of mixture of modulations given previously in [7] is generalized for different spectral efficiency values. As a result, Tables I, III and IV are provided for mixture of modulations. From Fig. 2(b), as α increases less, time is allocated for the information processing $((1-\alpha)T/2)$ per link. As a result, by increasing the α value, we need to increase the modulation order to maintain the same spectral efficiency, namely, the same total number of the transmitted bits for a fair BER comparison among three protocols. However, it turns out that not for every value of α an M -(QAM/PSK) modulation scheme is possible (M has to be an integer power of 2). Therefore, we have considered mixture of two modulations schemes to maintain the same spectral efficiency. In Tables I, III and IV, mixture of modulations are calculated for different rates (bits/sec/Hz). Furthermore, in these tables, α begins by considering small values and lower modulation orders (more information processing time) while higher α values correspond to higher order modulations (less information processing time).

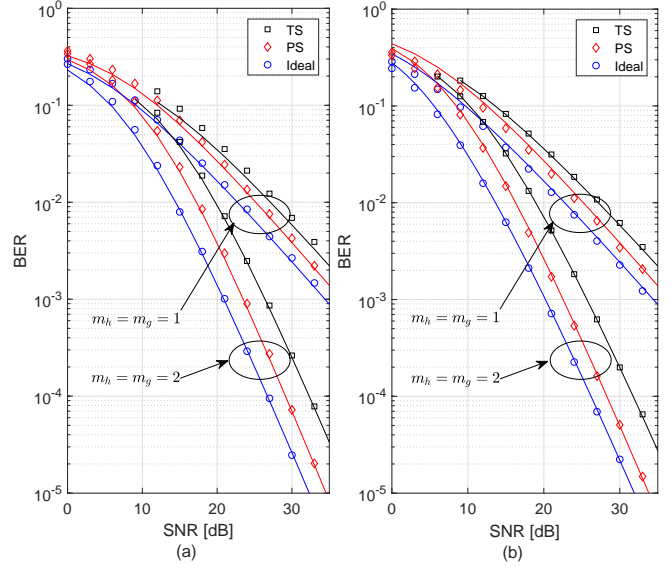


Fig. 3. DH system end-to-end BER performance versus SNR for $d_1 = d_2 = 0.5$ and $R = 1$, (a) AF and (b) DF.

As an example, when $\alpha = 1/7$, the necessary bandwidth is determined by the $R \rightarrow D$ transmission interval of $3T/7$ seconds, which is lower than that of $S \rightarrow R$ transmission. In order to maintain the spectral efficiency of $R = 1$ bits/sec/Hz, we should transmit 7 bits by 3 symbols during T seconds, namely, by two 4-QAM symbols each transmitting 2 bits and one 8-QAM symbol transmitting 3 bits. The necessary bandwidth is $(\frac{3T}{7 \times 3})^{-1} = \frac{7}{T}$ Hz and the spectral efficiency is $R = (2 \times (2/3) + 3 \times (1/3)) \times (3/T)/(7/T) = 1$ bit/sec/Hz³.

Figs. 3(a) and 3(b) depict the BER of DH-AF and DH-DF systems, respectively, for $d_1 = d_2 = 0.5$. In Fig. 3, for each SNR value, the corresponding optimum ρ or α values are numerically calculated as shown in Fig. 4. These optimum values are applied to obtain the curves given in Fig. 3 for PS and TS protocols. From Figs. 3(a) and 3(b), PS provides approximately 3 and 4 dB gains in SNR compared to TS, for the BER values of 10^{-2} and 10^{-3} , respectively, for both $m_h = m_g = 1$ and $m_h = m_g = 2$ cases. Furthermore, for $m_h = m_g = 1$, DF and AF system performances are nearly equivalent for all protocols, which is consistent with the results given in [27] for the non-EH DH system. However, when $m_h = m_g = 2$ for which the impact of AWGN increases, DF provides better performance than AF because of decoding at the relay, which avoids forwarding the noisy version of the signal.

It is shown in Fig. 3 that for the TS case, for both DF and AF systems, the results are given for SNR values approximately higher than 10 dB. We observe from Fig. 4 that, in TS protocol, for both AF and DF relaying, the optimum value of α is equal to $5/7$ when the SNR value is below 9 dB and 6 dB and, 6 dB and 4 dB for $m_h = m_g = 1$ and $m_h = m_g = 2$ cases, respectively. However, for above these SNR values,

³Note that in Tables. I, III and IV, M_p stands for 2^p -QAM (PSK) constellation.

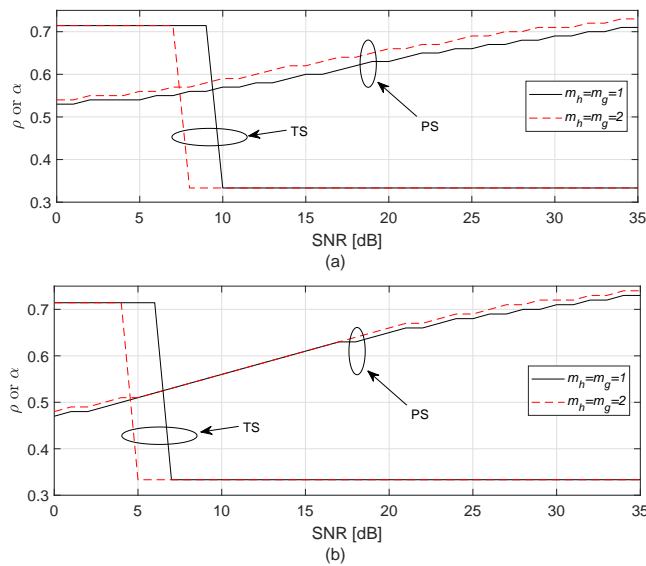


Fig. 4. Optimum ρ and α values in terms of minimum BEP for $d_1 = d_2 = 0.5$ and $R = 1$, (a) AF and (b) DF.

the optimum α is equal to $1/3$. From Table I, for $R = 1$, the corresponding modulation schemes are 128-QAM when $\alpha = 5/7$ and 8-QAM when $\alpha = 1/3$. On the other hand, since we have assumed the common approximation of $P_b \simeq P_s/k$, which is valid for the high SNR, at low SNR values where a higher modulation order (128-QAM for $\alpha = 5/7$) is required (as can be seen from Figs. 4(a) and 4(b)), the computer simulation and theoretical results do not match perfectly with each other. Therefore, the corresponding SNR values for 128-QAM have not been considered in Fig. 3 for both AF and DF systems. However, the results are given for SNR values for which $\alpha = 1/3$ and 8-QAM is employed. Finally, for PS and ideal protocols, the curves in Fig. 3 have been given for SNR values above 0 dB since for these protocols, the same spectral efficiency value ($R = 1$) is achieved with a lower modulation order (4-QAM).

In Figs. 4(a) and 4(b), the optimum ρ and α values, which minimize the BEP, are depicted with respect to SNR for DH-AF and DH-DF systems, respectively. From these curves we conclude that for PS protocol, the optimum value of ρ increases from 0.54 to 0.72 and from 0.47 to 0.73 for AF and DF, respectively, when SNR increases from 0 to 35 dB. We observe that, in TS protocol, for both AF and DF, the optimum value of α is equal to $5/7$ when the SNR value is below 9 dB and 6 dB and, 6 dB and 4 dB for $m_h = m_g = 1$ and $m_h = m_g = 2$ cases, respectively. However, for above these SNR values, the optimum α is equal to $1/3$. From Table I, for $R = 1$, the corresponding modulation schemes are 128-QAM (PSK) when $\alpha = 5/7$ and 8-QAM (PSK) when $\alpha = 1/3$. Note that since the optimization for TS protocol is performed for specific values of α , the resulting curves are discontinuous for both AF and DF cases in Fig. 4.

Figs. 5 and 6 show the BER performances of DH-AF and DH-DF systems versus ρ and α , respectively, for the parameters of $d_1 = d_2 = 0.5$, SNR = 30 dB and $R = 1$. For

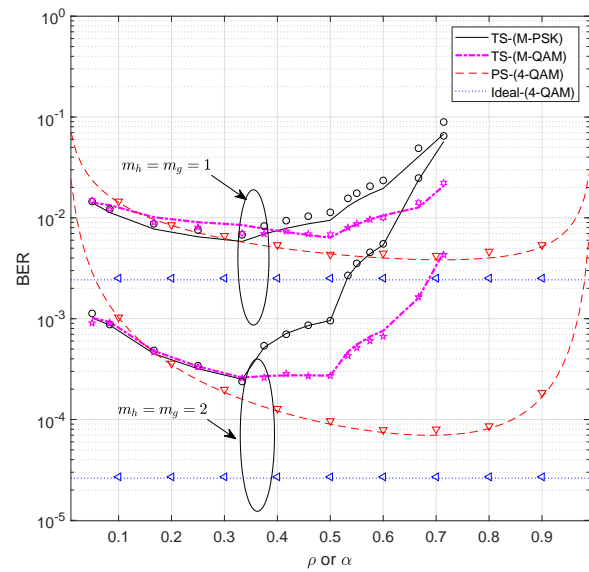


Fig. 5. DH-AF system end-to-end BER performance versus ρ and α for SNR = 30 dB, $d_1 = d_2 = 0.5$ and $R = 1$.

comparison purposes, the BER curves of the ideal protocol are also depicted in these figures for PS and TS protocols. For channel parameter values $m_h = m_g = 1$, DH-AF and DH-DF systems provide approximately the same performance while for $m_h = m_g = 2$, DH-DF system outperforms DH-AF system. From Figs. 5 and 6, for TS protocol when $R = 1$, the optimum α value for both DH-DF and DH-AF systems is equal to $1/3$, which corresponds to 8-QAM (PSK) modulation from Table I. However, for PS and ideal protocols, the employed modulation is 4-QAM and independent of ρ . Note that for TS, BER curves are not smooth due to the use of different modulation levels for different α values to maintain the spectral efficiency at a fixed value. Moreover, PS gives better BER performance compared to TS when $\rho > 1/3$ and $\rho > 0.2$ for the $m_h = m_g = 1$ and $m_h = m_g = 2$ cases, respectively, for both AF and DF relaying. Furthermore, theoretical and computer simulation results perfectly match for PS, TS and ideal protocols.

In Fig. 7, BER performance is provided with respect to d_1 for PS, TS and ideal protocols. For each d_1 value, the optimum α and ρ values are employed in Fig. 7 for both systems. The results show that $d_1 = 0.5$ gives the optimum BER for both DH-AF and DH-DF systems. In case of $R = 1$, for PS and ideal protocols, the employed modulation is 4-QAM and independent of ρ while for TS protocol, $\alpha = 1/3$ gives the optimum results for both DH-AF and DH-DF systems and all values of d_1 , where $R = 1$ corresponds to 8-QAM. From Figs. 7(a) and 7(b), it is concluded that PS protocol provides better performance than TS for both AF and DF cases.

Fig. 8 shows the BER performance with respect to the channel parameter m_h for two fixed m_g values and $R = 1$, where the optimum ρ and α values are applied. From the theoretical and simulation results, it is concluded that the BER performances of the DH-AF and DH-DF systems are

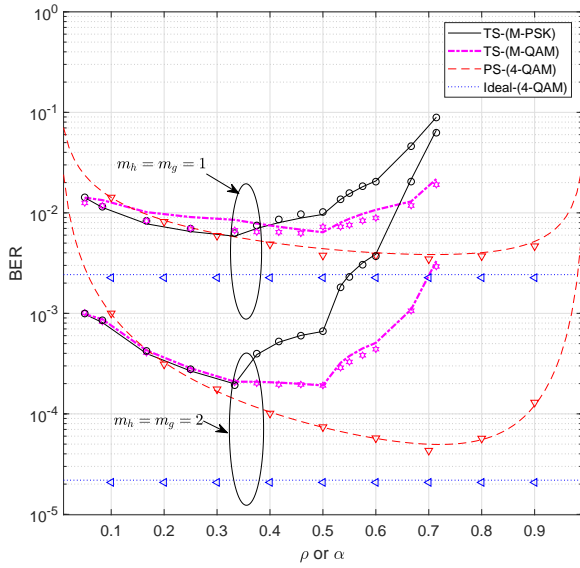


Fig. 6. DH-DF system end-to-end BER performance versus ρ and α for SNR = 30 dB, $d_1 = d_2 = 0.5$ and $R = 1$.

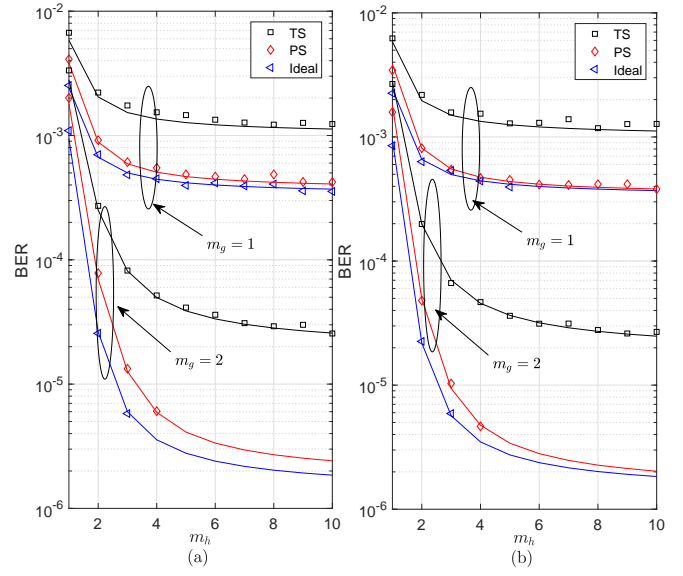


Fig. 8. DH system end-to-end BER performance versus m_h for SNR = 30 dB, $d_1 = d_2 = 0.5$ and $R = 1$, (a) AF and (b) DF.

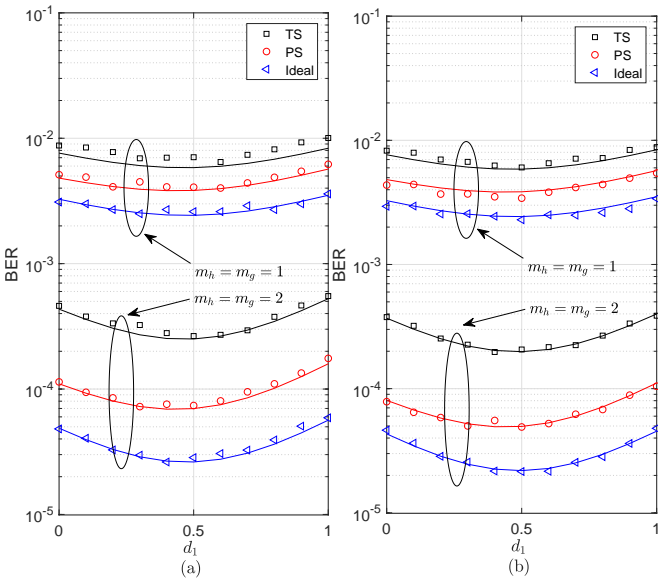


Fig. 7. DH system end-to-end BER performance versus d_1 for SNR = 30 dB, $R = 1$ and $(d_1 + d_2 = 1)$. (a) AF and (b) DF.

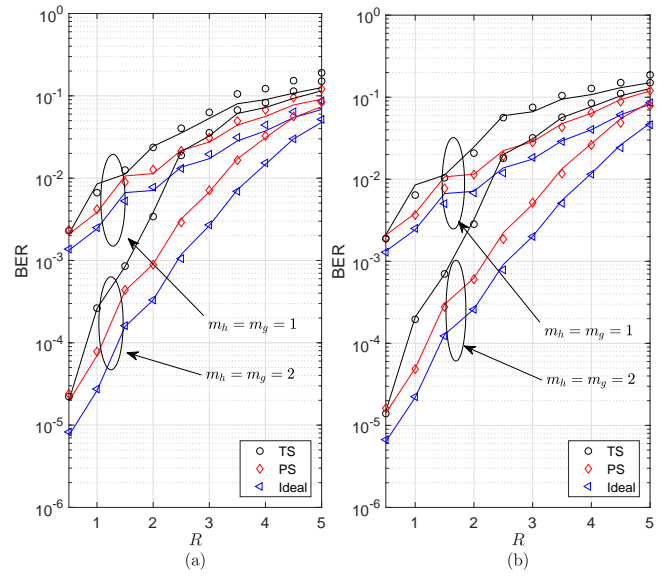


Fig. 9. DH system end-to-end BER performance versus R for SNR = 30 dB, $d_1 = d_2 = 0.5$ and M -QAM, (a) AF and (b) DF.

approximately equivalent for $m_g = 1$, however, for $m_g = 2$, DH-DF system slightly outperforms DH-AF. PS protocol provides better performance than TS since higher values of the channel parameters enable the relay to correctly decode the received signal and to harvest much more energy.

The BER performances of DH-AF and DH-DF systems versus R for different system parameter values are given in Figs. 9(a) and 9(b), respectively. In this figure, M -QAM is considered since it outperforms M -PSK for $M > 4$. Also, the BER curve of the ideal protocol is depicted in this figure for comparison purposes. For each value of R , these curves are obtained for corresponding optimum values

of ρ and α . From Figs. 9(a) and 9(b), we observe that PS outperforms TS for both DH-AF and DH-DF systems, where the maximum difference between two systems are obtained when $R = 2.5$. Moreover, due to our approximation in (20), increasing R results in increased modulation order for which the approximation in (20) becomes loose, especially when $m_h = m_g = 1$, for both DH-AF and DH-DF systems.

V. CONCLUSION

In this paper, we have considered the energy harvesting issue in a conventional DH relaying network where the relay applies PS, TS and ideal protocols with AF/DF relaying tech-

niques to harvest energy from the received RF source signal and to transmit it to the destination with the harvested energy. Tight closed-form analytical expressions for the BEP of both DH-AF and DH-DF systems have been derived and approved by the computer simulations. Moreover, since IP time interval varies in TS protocol with respect to the parameter α , the mixture of modulations technique has been applied to maintain a constant spectral efficiency level. Finally, optimal values of the system parameters, which minimize BEP, have been obtained for both DH-AF and DH-DF systems. Our work has shed light on the BER performance of AF and DF-aided DH networks employing EH and provided guidelines for the system designer. An adaptive selection of time slots for EH systems can be considered as a future work.

APPENDIX A

PDF OF THE PRODUCT OF TWO CHI-SQUARE DISTRIBUTED RANDOM VARIABLES

The PDF of random variable $Z = |h|^2|g|^2$ is given in [23, 6.148] as

$$f_Z(z) = \int_0^\infty \frac{1}{x} f_{|h|^2}(x) f_{|g|^2}\left(\frac{z}{x}\right) dx \quad (25)$$

where for $i \in \{h, g\}$, [28, 2.3.21]

$$f_{|i|^2}(x) = \left(\frac{m_i}{\Omega_i}\right)^{m_i} \frac{x^{m_i-1}}{\Gamma(m_i)} \exp(-xm_i/\Omega_i). \quad (26)$$

Substituting (26) in (25), after simplification and using [21, 3.478.4] we have

$$f_Z(z) = 2F \left(\frac{m_g \Omega_h}{\Omega_g m_h} \right)^{\Omega/2} z^{\epsilon-1} K_\Omega \left(2\sqrt{\frac{m_h m_g}{\Omega_h \Omega_g}} z \right) \quad (27)$$

where m_h and m_g are the Nakagami fading parameters and $\Omega_h = E[|h|^2]$, $\Omega_g = E[|g|^2]$, $\Omega = m_h - m_g$, $\epsilon = 0.5(m_h + m_g)$ and $F = (m_h/\Omega_h)^{m_h} (m_g/\Omega_h)^{m_g} \Gamma(m_h)^{-1} \Gamma(m_g)^{-1}$.

APPENDIX B

CDF OF THE SNR IN AF STRATEGY

The received SNR at the destination for AF relaying is given as

$$\gamma = \frac{A|h|^4|g|^2}{B|h|^2|g|^2 + C|h|^2 + D} \quad (28)$$

where the constants A, B, C and D differ for PS, TS and ideal protocols. For high SNR, taking $D = 0$, (28) can be rewritten as

$$\gamma \simeq \frac{AXY}{BX + C} \quad (29)$$

where $Y = |h|^2$ and $X = |g|^2$. Using [23, Chap. 6], the CDF of γ can be calculated as

$$F_\gamma(\gamma) = \int_0^\infty F_Y\left(\frac{\gamma}{A}\left(B + \frac{C}{X}\right) | X\right) f_X(x) dx. \quad (30)$$

Assuming that the channels are exposed to Nakagami- m fading, CDF of the channel gain is given in [28, 2.3.24] as

$$F_Y(y) = 1 - \exp(-ym_h/\Omega_h) \sum_{k=0}^{m_h-1} \frac{1}{k!} \left(\frac{ym_h}{\Omega_h}\right)^k. \quad (31)$$

Substituting (26) and (31) in (30) and using a binomial expansion [21, Eq. 1.111] and [21, Eq. 3.471.9], after some simplification, CDF of γ can be written as

$$F_\gamma(\gamma) = 1 - \frac{2}{\Gamma(m_g)} \sum_{k=0}^{m_h-1} \sum_{i=0}^k T(k, i) \Lambda(k, i, \gamma) \quad (32)$$

where

$$T(k, i) = \frac{1}{(k-i)!} \left(\frac{m_h}{\Omega_h A}\right)^\kappa \left(\frac{C m_g}{\Omega_g}\right)^{\frac{m_g+i}{2}} B^{k-i},$$

$$\Lambda(k, i, \gamma) = \exp\left(-\frac{m_h B}{\Omega_h A} \gamma\right) \gamma^\kappa K_{m_g-i} \left(2\sqrt{\frac{m_h m_g C}{\Omega_h \Omega_g A}} \gamma\right)$$

and $\kappa = (m_g - i + 2k)/2$, respectively.

REFERENCES

- [1] L. R. Varshney, "Transporting information and energy simultaneously," in *Proc. 2008 IEEE Int. Symp. on Info. Theo.*, July 2008, pp. 1612–1616.
- [2] P. Grover and A. Sahai, "Shannon meets Tesla: Wireless information and power transfer," in *Proc. 2010 IEEE Int. Symp. on Info. Theo.*, June 2010, pp. 2363–2367.
- [3] A. A. Nasir, X. Zhou, S. Durrani, and R. A. Kennedy, "Relaying protocols for wireless energy harvesting and information processing," *IEEE Trans. Wireless Commun.*, vol. 12, no. 7, pp. 3622–3636, July 2013.
- [4] X. Zhou, R. Zhang, and C. K. Ho, "Wireless information and power transfer: Architecture design and rate-energy tradeoff," *IEEE Trans. Commun.*, vol. 61, no. 11, pp. 4754–4767, Nov. 2013.
- [5] A. A. Nasir, X. Zhou, S. Durrani, and R. A. Kennedy, "Throughput and ergodic capacity of wireless energy harvesting based DF relaying network," in *Proc. 2014 IEEE Int. Conf. Commun. (ICC)*, June 2014, pp. 4066–4071.
- [6] Z. Mheich and V. Savin, "Cooperative communication protocols with energy harvesting relays," in *2017 Wireless Days*, Mar. 2017, pp. 60–65.
- [7] C. Huang, P. Sadeghi, and A. A. Nasir, "BER performance analysis and optimization for energy harvesting two-way relay networks," in *2016 Australian Commun. Theo. Workshop (AusCTW)*, Jan. 2016, pp. 65–70.
- [8] R. Tao, A. Salem, and K. A. Hamdi, "Adaptive relaying protocol for wireless power transfer and information processing," *IEEE Commun. Lett.*, vol. 20, no. 10, pp. 2027–2030, Oct. 2016.
- [9] N. P. Le, N. S. Vo, and M. T. Hoang, "Throughput analysis of energy harvesting MIMO relay systems over Nakagami-m fading channels," in *Proc. 2017 Int. Conf. on Recent Advances in Signal Process., Telecommun. Comput. (SigTelCom)*, Jan. 2017, pp. 164–169.
- [10] Z. Zhou, M. Peng, Z. Zhao, and Y. Li, "Joint power splitting and antenna selection in energy harvesting relay channels," *IEEE Signal Process. Lett.*, vol. 22, no. 7, pp. 823–827, July 2015.
- [11] Y. Gu and S. Assa, "RF-based energy harvesting in decode-and-forward relaying systems: Ergodic and outage capacities," *IEEE Trans. Wireless Commun.*, vol. 14, no. 11, pp. 6425–6434, Nov. 2015.
- [12] H. Chen, X. Zhou, Y. Li, P. Wang, and B. Vucetic, "Wireless-powered cooperative communications via a hybrid relay," in *2014 IEEE Info. Theo. Workshop (ITW 2014)*, Nov. 2014, pp. 666–670.
- [13] S. Guo, H. Zhang, Y. Wang, and D. Yuan, "Spatial modulated simultaneous wireless information and power transfer," in *Proc. 2016 IEEE Global Commun. Conf. (GLOBECOM)*, Dec 2016, pp. 1–6.
- [14] M. Zhang and X. Cheng, "Spatial-modulation-based wireless-powered communication for achievable rate enhancement," *IEEE Commun. Lett.*, vol. 21, no. 6, pp. 1365–1368, June 2017.
- [15] D. D. Tran, H. V. Tran, D. B. Ha, H. Tran, and G. Kaddoum, "Performance analysis of two-way relaying system with RF-EH and multiple antennas," in *Proc. 2016 IEEE 84th Veh. Technol. Conf. (VTC-Fall)*, Sept. 2016, pp. 1–5.
- [16] Y. Liu, L. Wang, M. Elkashlan, T. Q. Duong, and A. Nallanathan, "Two-way relaying networks with wireless power transfer: Policies design and throughput analysis," in *Proc. 2014 IEEE Global Commun. Conf.*, Dec. 2014, pp. 4030–4035.
- [17] C. Zhang, H. Du, and J. Ge, "Energy-efficient power allocation in energy harvesting two-way AF relay systems," *IEEE Access*, vol. 5, pp. 3640–3645, 2017.

[18] Y. Gu, H. Chen, Y. Li, and B. Vucetic, "Wireless-powered two-way relaying with power splitting-based energy accumulation," in *Proc. 2016 IEEE Global Commun. Conf. (GLOBECOM)*, Dec 2016, pp. 1–6.

[19] N. T. P. Van, S. F. Hasan, X. Gui, S. Mukhopadhyay, and H. Tran, "Three-step two-way decode and forward relay with energy harvesting," *IEEE Commun. Lett.*, vol. 21, no. 4, pp. 857–860, Apr. 2017.

[20] Z. Ding, I. Krikidis, B. Sharif, and H. V. Poor, "Wireless information and power transfer in cooperative networks with spatially random relays," *IEEE Trans. Wireless Commun.*, vol. 13, no. 8, pp. 4440–4453, Aug. 2014.

[21] A. Jeffrey and D. Zwillinger, *Table of Integrals, Series, and Products*. Academic press, 2007.

[22] M. Simon and M. Alouini, *Digital Communication over Fading Channels*, 2nd ed. Wiley, 2005.

[23] A. Papoulis and S. Pillai, *Probability, Random Variables, and Stochastic Processes*, 4th ed. McGraw-Hill, 2002.

[24] R. H. Y. Louie, Y. Li, and B. Vucetic, "Practical physical layer network coding for two-way relay channels: performance analysis and comparison," *IEEE Trans. on Wireless Commun.*, vol. 9, no. 2, pp. 764–777, Feb. 2010.

[25] Wolfram. (2001) The Wolfram functions site. Internet. [Online], <http://functions.wolfram.com>.

[26] V. S. Adamchik and O. I. Marichev, "The algorithm for calculating integrals of hypergeometric type functions and its realization in reduce system," in *Proc. of the Int. Symp. on Symbolic and Algebraic Comput.*, ser. ISSAC '90, 1990, pp. 212–224.

[27] M. O. Hasna and M. S. Alouini, "End-to-end performance of transmission systems with relays over Rayleigh-fading channels," *IEEE Trans. Wireless Commun.*, vol. 2, no. 6, pp. 1126–1131, Nov. 2003.

[28] J. G. Proakis, *Digital Communications*, 5th ed. McGraw-Hill, 1995.



Ertugrul Basar (S'09-M'13-SM'16) was born in Istanbul, Turkey, in 1985. He received the B.S. degree (Hons.) from Istanbul University, Turkey, in 2007, and the M.S. and Ph.D. degrees from Istanbul Technical University, Turkey, in 2009 and 2013, respectively. From 2011 to 2012, he was with the Department of Electrical Engineering, Princeton University, Princeton, NJ, USA, as a Visiting Research Collaborator. He was an Assistant Professor with Istanbul Technical University from 2014 to 2017, where he is currently an Associate Professor of Electronics and Communication Engineering. His primary research interests include MIMO systems, index modulation, cooperative communications, OFDM, and visible light communications.

Recent recognition of his research includes the Young Scientists Award of the Science Academy (Turkey) in 2018, Turkish Academy of Sciences Outstanding Young Scientist Award in 2017, the first-ever IEEE Turkey Research Encouragement Award in 2017, and the Istanbul Technical University Best Ph.D. Thesis Award in 2014. He is also the recipient of four Best Paper Awards including one from the IEEE International Conference on Communications 2016. Dr. Basar currently serves as an Editor of the IEEE TRANSACTIONS ON COMMUNICATIONS and *Physical Communication* (Elsevier), and as an Associate Editor of the IEEE COMMUNICATIONS LETTERS and the IEEE ACCESS.



Mohammadreza Babaei (S'11) received his B.S. degree from Tabriz University, Tabriz, Iran, in 2011, and M.S. degree from Istanbul Technical University, Istanbul, Turkey, in 2016. He is currently a Ph.D. student and a member of Wireless communication laboratory in Istanbul Technical University, Istanbul, Turkey. He has served as a TPC member for several IEEE conferences and as a reviewer for IEEE journals. His research interests include MIMO systems, cognitive radio, cooperative communications, spatial modulation, energy harvesting and NOMA.



Ümit Aygölü received his B.S., M.S. and Ph.D. degrees, all in electrical engineering, from Istanbul Technical University, Istanbul, Turkey, in 1978, 1984 and 1989, respectively. He was a Research Assistant from 1980 to 1986 and a Lecturer from 1986 to 1989, at Yildiz Technical University, Istanbul, Turkey. In 1989, he became an Assistant Professor at Istanbul Technical University where he became an Associate Professor and Professor in 1992 and 1999, respectively. His current research interests include MIMO systems, cooperative communications, cognitive radio, spatial modulation, energy harvesting and NOMA.